Genetic Analysis Of Programmed Cell Death

by

Grace Kathryn Alexander

A Paper Presented to the

Faculty of Mount Holyoke College in

Partial Fulfillment of the Requirements for

the Degree of Bachelors of Arts with

Honor

Department of Biological Sciences

Mount Holyoke College

South Hadley, MA 01075

May 2021

This paper was prepared

under the direction of

Professor Craig Woodard

for eight credits.

For my Grandfather

Acknowledgements

I would like to extend my deepest thanks to my mentor, Professor Craig Woodard, for his guidance, expertise, and confidence in me. My time in his lab has been my defining experience at Mount Holyoke College, growing me both academically and personally, and shaping my vision of my professional future. Thank you for your wisdom and encouragement. I look up to you greatly, and hope to follow in your footsteps.

I would like to thank my fellow Woodard Lab members for their support, and for making this as wonderful an experience as it has been. I would especially like to thank Marlena Starrs for accompanying me on late-night lab trips and fly food cooking adventures, and for being one of my most enthusiastic supporters in the lab. I value our friendship, and wish you luck as you continue your own research.

I would also like to thank the other members of my thesis committee, Professor Sarah Bacon and Professor Margaret Robinson. You are wonderful professors from whom I feel I have learned greatly, and your continued support of me both in the classroom and beyond means a lot to me. I hope to be as inspiring, encouraging, and nurturing as you have been to me.

Lastly, I would like to thank Mount Holyoke College and the Department of Biological Sciences for making this research possible.

Table of Contents

Acknowledgements **4**

Table of Contents **5**

List of Figures **7**

List of Tables **8**

Abstract **9**

Introduction **10**

I. Programmed Cell Death 10

Biological Function 10

Misregulation 12

II. *Drosophila melanogaster* 13

Background and Life Cycle 13

Larval Fat Bodies 15

III. *Drosophila* Metamorphosis and the PCD Pathway 17

20-Hydroxyecdysone 17

ßFTZ-F1 20

Diap1, *Dronc*, and the PCD Signaling Pathway 22

IV. Real-Time Quantitative Reverse Transcription Polymerase Chain Reaction 25

V. Findings of Previous Experiments 27

VI. Hypothesis and Goals of this Study 28

Materials and Methods: Preliminary Research **29**

I. RNA Isolation 29

II. First-Strand cDNA Synthesis 30

III. Reverse Transcriptase PCR and Gel Electrophoresis 31

Results **35**

I. RNA Isolation 35

II. Gel Electrophoresis 36

Discussion **38**

I. Preliminary Research 38

II. Current and Continuing Research 38

III. Conclusion 39

Appendix **41**

Literature Cited **42**

List of Figures

Figure 1. Visualization of morphological changes during apoptosis 11

Figure 2. Life cycle of *Drosophila melanogaster*. 14

Figure 3. Progression of larval fat body dissociation 14

Figure 4. 20-hydroxyecdysone 17

Figure 5. EcR/USP activation of ecdysone-induced genes 18

Figure 6. Timing of ecdysone pulses and expression of *ßFTZ-F1* 20

Figure 7. Regulation of the larval salivary gland PCD pathway 23

Figure 8. qRT-PCR with fluorescent dye 25

Figure 9. qRT-PCR quantitation 26

Figure 11. 10mm Absorbance vs. Wavelength in nm for RNA sample 10/22 35

Figure 12. 10mm Absorbance vs. Wavelength in nm for RNA sample 10/31 36

Figure 13. Gel electrophoresis of *Drosophila melanogaster* w^{1118} cDNA amplified with *Dronc* (C), *Actin 5c* (B), and *Diap1* (A) primers from samples 10/22 (1) and 10/31 (2) 37

List of Tables

Table 1. Master mix 1 reagents for cDNA synthesis 30
Table 2. Master mix 2 reagents for cDNA synthesis 31
Table 3. Forward and reverse primer sequences for *Diap1*, *Actin 5c*, and *Dronc* 32
Table 4. Reagents for RT-PCR 33
Table 5. RT-PCR Thermocycler profile for program *diap1primerset1* 33
Table 6. Labeling schematic for RT-PCR tubes 41

Abstract

The larval fat bodies of *Drosophila melanogaster* are responsible for storing energy from the larval feeding stages for use during pupal development (Agulia et al. 2007). In most larval tissues, programmed cell death (PCD) is triggered by two pulses of the steroid hormone 20-hydroxyecdysone (ecdysone), delivered at the end of the third larval instar stage and at 12 hours after puparium formation, respectively (Lee et al. 2002). Ecdysone signaling induces the transcription of the death activator genes, *rpr, hid,* and *grim,* which interact with the E3-ubiquitin ligase *Diap1* to give rise to PCD (Lee et al. 2002; Steller 2008; Yin & Thummel 2004). *Diap1* has been found to promote the degradation of the PCD initiator caspase *Dronc,* thus acting as an inhibitor of unwanted cell death (Steller 2008). Upon ecdysone-induced transcription, the death activator genes promote the auto-ubiquitination of *Diap1*, removing its inhibitory effect and triggering caspase activation (Hawkins et al. 2000; Lee et al. 2002; Steller 2008; Yin & Thummel 2004). Studies have shown that *Dronc* plays an essential role in the promotion of PCD, with its loss of function being associated with a decrease in necessary PCD (Fraser et al. 1997; Kumar & Doumanis 2000; Meier et al. 2000). Unlike other larval tissues, larval fat bodies are noted for their resistance to PCD, dissociating from a tissue to free, individual fat cells rather than undergoing PCD (Agulia et al. 2007). This study follows upon previously conducted research, hypothesizing that up-regulation of *Dronc* and down-regulation of *Diap1* promotes PCD in *Drosophila melanogaster,* and predicting that the PCD-resistant larval fat bodies will display up-regulation of *Diap1* and down-regulation of *Dronc* (Han 2019). This study plans to compare the relative levels of *Diap1* and *Dronc* in PCD-resistant larval fat bodies to those in the larval salivary glands, a PCD-susceptible larval tissue. Preliminary results indicate that this experiment can be done and that all primers and equipment are working as intended. Next steps include the analysis of cDNA synthesized from larval fat bodies and larval salivary glands collected from pupae at 12 hours after puparium formation via qRT-PCR. Understanding of the role of these expression levels in the regulation of PCD has broader implications for research into cancer development, degenerative diseases, and treatments thereof.

Introduction

I. Programmed Cell Death

Biological Function

Programmed Cell Death (PCD) is the biologically-regulated self-destruction of cells. The term PCD is often used to refer to apoptosis, a specific classification of cell death serving as a critical process of normal organismal development, in which self-destruction of the cell occurs without causing harm to neighboring cells or producing an inflammatory response (Kroemer et al. 2005; McGill & Fisher 1997). Apoptotic PCD is characterized by a series of biochemical events leading to retraction of pseudopodes, reduction in cellular volume, chromatin condensation, nuclear fragmentation, and plasma membrane blebbing, among other morphological changes (Chen & Lai 2009; Kroemer et al. 2005). Chromosomal DNA fragmentation may also be considered a hallmark of this particular classification of cell death, though it is possible for apoptosis to occur without it (Chen & Lai 2009; Kroemer et al. 2005). The activation of caspases as a component of the cell death program may potentially be the source of the distinctive apoptotic morphology, and can be useful in diagnosing whether PCD has occurred (Kroemer et al. 2005). Apoptotic PCD is unique amongst forms of cell death in its function of conferring developmental advantages on an organism, regulating cell numbers and interactions, playing a role in body plan differentiation during development, and removing extraneous or potentially harmful cells (Chen & Lai 2009; McGill & Fisher 1997). Though particularly critical to development, this important biological event continues to occur throughout an organism's life; in an adult human, 50 billion to 70 billion cells undergo apoptotic PCD every day, and it is estimated that an individual's body weight in cells are destroyed by

PCD in a year (Chen & Lai 2009). Apoptotic machinery is highly conserved, and while the specific triggers of the PCD pathway may vary across systems and species, apoptosis "effector pathways" have remained evolutionarily conserved across a wide variety of species, making it possible to investigate the mechanical underpinnings of the process by studying model organisms (McGill & Fisher 1997).

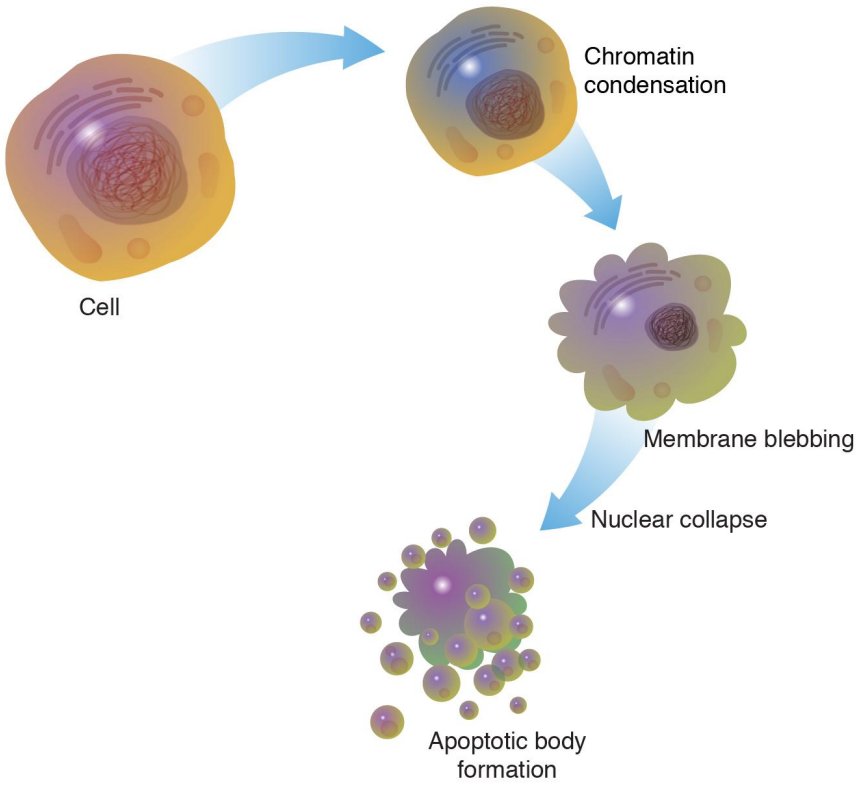

Figure 1. Visualization of morphological changes during apoptosis. Changes such as chromatin condensation, membrane blebbing, and nuclear fragmentation (here referred to as nuclear collapse) occur during this biological process (Austin (n.d.)).

Misregulation

Incorrectly timed PCD has been implicated as an underlying cause in a number of health conditions. In response to environmental and endogenous factors, the pathway regulating PCD may become uncontrolled, and may lead to the cell becoming anti-apoptotic, favoring resistance to PCD, or pro-apoptotic, favoring increased sensitivity to PCD (Chen & Lai 2009). Anti-apoptotic dysregulation is the subject of several studies in cancer research, as PCD resistance has been implicated as an underlying cause in tumorigenesis and cancer development (Chen & Lai 2009). It has been found that many known regulators of cell proliferation also serve as PCD inducers, however requiring a tumor suppressor to function as PCD promoters (McGill & Fisher 1997). Malignant tumor cells often exhibit mutations in PCD pathway components, circumventing apoptotic processes in order to metastasize (McGill & Fisher 1997). Furthermore, chemotherapies have been shown to function by activating apoptotic pathways, inducing the self-destruction of tumor cells (McGill & Fisher 1997). Understanding the underlying mechanisms of PCD has potential in the further development of cancer treatments, as increased knowledge of its pathways might yield improved means of inducing this process in cancer cells (Chen & Lai 2009). A 2009 collection of research into various cancer types in humans details different means of PCD regulation across tissue types, however it does not appear that at the time of this collection's assembly that any common points in these apoptotic pathways are well understood (Chen & Lai 2009). There are also studies suggesting that pro-apoptotic dysregulation of PCD may be linked to neurodegenerative disorders, such as Alzheimer's disease, Parkinson's disease, Huntington's disease, stroke, and amyotrophic lateral sclerosis (ALS) (Mattson 2000). In one study, the unusual loss of neuronal cells observed in Alzheimer's disease was shown to be due to PCD following the degeneration of cells, and in another,

apoptotic PCD has been found to occur in the midbrains of patients with Parkinson's disease (LaFerla et al. 1995; Mochizuki et al. 1996). As neuronal tissues maintain their function and complexity by not undergoing cell division, which leads to PCD in most other tissues, the post-mortem observation of PCD in tissues exhibiting neurodegenerative disorders helps to implicate pro-apoptotic dysregulation in a handful of neurodegenerative diseases (Mattson 2000). It has been suggested that identifying and blocking the apoptotic triggers leading to PCD in each of these neurodegenerative disorders may help to treat them, though the effectiveness of this approach is not guaranteed (Mattson 2000).

II. *Drosophila melanogaster*

Background and Life Cycle

The fruit fly *Drosophila melanogaster* is a useful model organism for analyzing the molecular genetic mechanisms underlying PCD. A few important discoveries have allowed for its continued use in research into human biology, genetics, and medicine (Jennings 2011). Estimated to be about 176 megabase pairs (Mbs) long, several iterations of the complete *Drosophila* genome have been reported, allowing for extensive genetic analysis thereof, and making it possible to employ a wide variety of research techniques across many different biological fields (Fernández-Moreno et al. 2007). Many of the key genes and biochemical pathways in *Drosophila* are evolutionarily conserved across all animals, allowing them to serve as a model granting insight into these processes in humans (Jennings 2011). Furthermore, the short lifespan and rapid population proliferation of *Drosophila* make it possible to raise and observe large populations for experimentation over a very brief period of time (Fernández-Moreno et al. 2007; Jennings 2011).

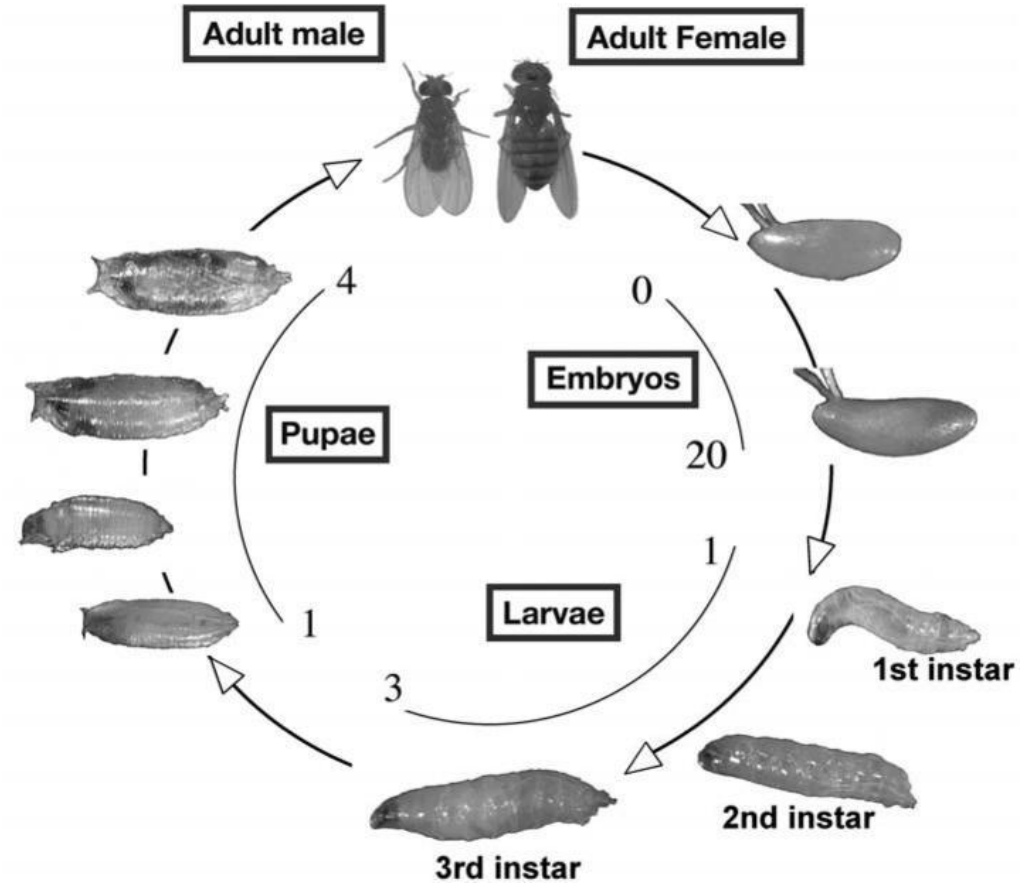

Figure 2. Life cycle of *Drosophila melanogaster*. The embryo stage is shown in approximate number of hours, while the larval and pupal stages are shown in approximate number of days (Fernández-Moreno et al. 2007).

The *Drosophila* life cycle consists of four distinct stages: Embryonic, larval, pupal, and adult (Fernández-Moreno et al. 2007; Jennings 2011). Of particular importance to this study are the larval stage and the pupal stage. The larval stage lasts for a total of five days, during which the larva feeds and accumulates reserves of nutrients for use during metamorphosis (Agulia et al. 2007; Jennings 2011). This stage features juvenile-specific tissues, known as larval tissues, specialized to aid in feeding and energy storage. *Drosophila* larvae undergo three stages, known as instars, the third and final of which is characterized by the start of the non-feeding period, beginning 24 to 48 hours before puparium formation and persisting until metamorphosis is

complete (Agulia et al. 2007; Fernández-Moreno et al. 2007; Jennings 2011). The *Drosophila* pupal stage lasts for approximately four days, during which metamorphosis occurs. (Fernández-Moreno et al. 2007). The 12 hours immediately following puparium formation are referred to as the prepupal stage, during which the majority of larval tissues undergo PCD so that they do not persist into the adult form (Bond et al. 2011; Fernández-Moreno et al. 2007; Jennings 2011).

Larval Fat Bodies

Among the larval tissues found in *Drosophila melanogaster* are the larval fat bodies, sheets of one-cell thick fat tissue arising from the embryonic mesoderm (Miller et al. 2002). Larval fat bodies play a critical role in the *Drosophila* life cycle, serving functions in metabolism, detoxification, immune response, and, most notably, energy storage (Agulia et al. 2007; Miller et al. 2002). Functioning as energy reserves, the larval fat bodies are responsible for the storage of energy from the larval feeding periods for use during the non-feeding period and metamorphosis (Agulia et al. 2007). As a result of this vital function, larval fat bodies exhibit an unusual resistance to PCD, having been found to persist into the adult stage where they continue to supply the newly-formed fly with energy until it has fed (Agulia et al. 2007).

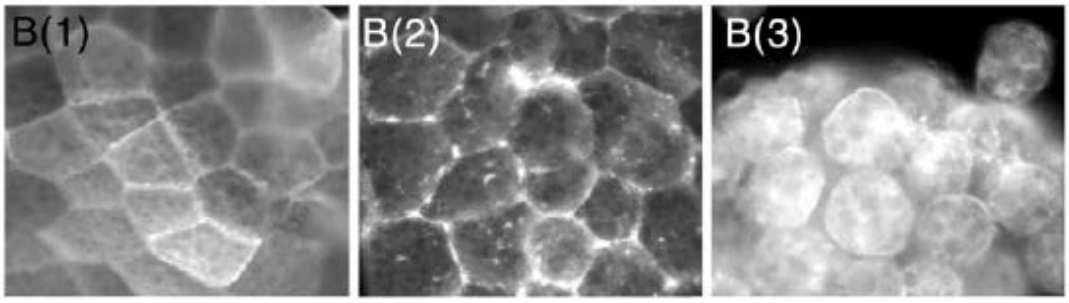

Figure 3. Progression of larval fat body dissociation. Fully-associated larval fat body sheets are shown in B(1); rounded, partially dissociated larval fat cells are shown in B(2); and a clump of fully dissociated individual larval fat cells is shown in B(3) (Bond et al. 2011).

Instead of destruction via PCD, the larval fat bodies undergo structural remodeling, dissociating from a sheet of tissue into clusters of individual fat cells (Nelliot et al. 2006). Morphological changes begin in the larval fat bodies during the prepupal stage (Nelliot et al. 2006). Between 4 to 6 hours after puparium formation (APF), the polygonal larval fat cells become rounded as the larval epidermis separates from the puparium (Nelliot et al. 2006). As prepupal development progresses, cells in the tissue sheet become less tightly associated (Nelliot et al. 2006). Full dissociation of the larval fat bodies occurs during the prepupal to pupal transition, at approximately 12 hours APF, regulated by the same developmental signal that gives rise to PCD in most other larval tissues (Bond et al. 2011; Nelliot et al. 2006). Both stages of dissociation occur in an anterior to posterior wave through the body (Nelliot et al. 2006). This dissociative process is carried out by matrix metalloproteinases (MMPs), a class of protease enzymes that target and cleave the extracellular matrix and its signalling molecules, increasing cell spacing and mobility (Bond et al. 2011). There are two MMPs involved in Drosophila larval fat body remodeling, MMP1 and MMP2, expressed at the prepupal to pupal transition (Bond et al. 2011). The expression of MMP2 in particular at this point in development has been found to be necessary for the proper remodeling of the larval fat bodies (Bond et al. 2011).

III. *Drosophila* Metamorphosis and the PCD Pathway

20-Hydroxyecdysone

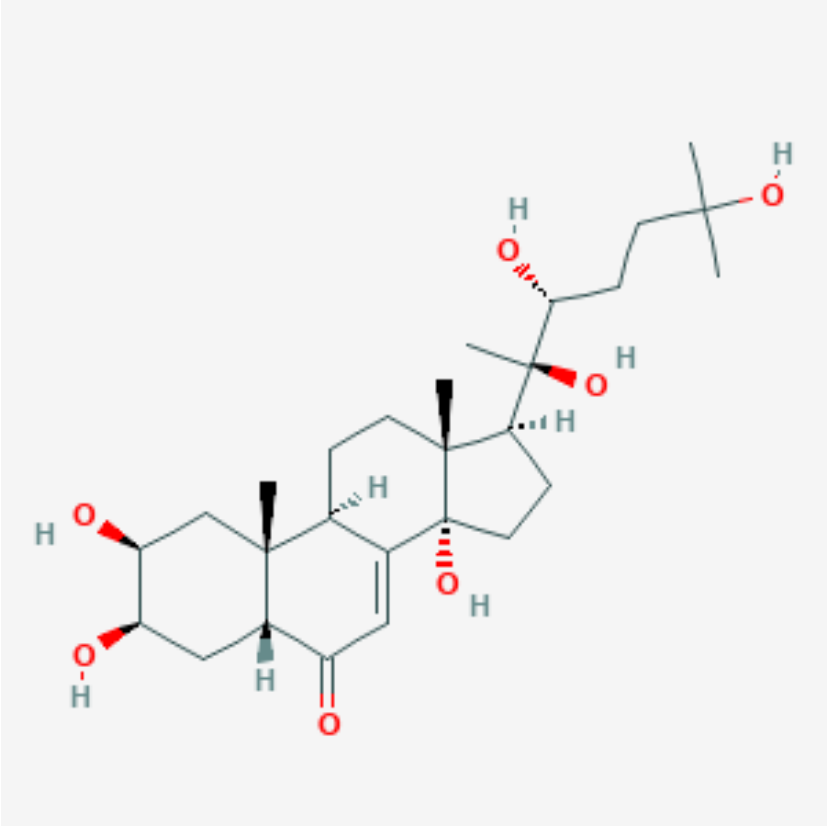

Figure 4. 20-hydroxyecdysone. The chemical structure of active form 20-hydroxyecdysone, consisting of three six-membered rings and one five-membered ring (NCBI 2021).

20-hydroxyecdysone is the active form of the steroid hormone ecdysone, a master regulator of development in insects such as *Drosophila melanogaster* (Yamanaka et al. 2013). As both 20-hydroxyecdysone and ecdysone are commonly referred to as ecdysone, "ecdysone" hereby denotes the active 20-hydroxyecdysone, and ecdysone in its inactive form will be referred to as "inactive ecdysone." During the larval stage, inactive ecdysone is synthesized from dietary cholesterol in the prothoracic gland, a *Drosophila* endocrine gland encoding ecdysone biosynthetic enzymes and substrate-trafficking molecules (Nakagawa & Sonobe 2016;

Yamanaka et al. 2013). Upon secretion into the hemolymph and peripheral nonendocrine cells including the larval fat bodies, inactive ecdysone is oxidized to its active form by the cytochrome P450 monooxygenases (Nakagawa & Sonobe 2016; Yamanaka et al. 2013). Ecdysone serves to initiate gene expression cascades during insect development, including the signaling cascades that govern *Drosophila* metamorphosis (Nakagawa & Sonobe 2016; Yamanaka et al. 2013). In developmental metamorphic regulation, ecdysone binds to the ecdysone receptor complex, a heterodimer comprised of two nuclear receptors: EcR and Ultraspiracle (USP) (Bond et al. 2011; Nakagawa & Sonobe 2016; Yamanaka et al. 2013; Zhu et al. 2006). Responsible for gene expression mediation of most known ecdysone-dependent genes, the EcR/USP complex initiates tissue-specific transcriptional cascades, allowing for certain tissues - notably, the larval fat bodies - to undergo stage-specific developmental changes (Bond et al. 2011; Yamanaka et al. 2013; Zhu et al. 2006). The EcR/USP complex directly activates the primary response genes, or early genes, which in turn undergo self-imposed repression in order to induce transcription of the prepupal late genes, amplifying ecdysone signals (Bond et al. 2011; Lee et al. 2002).

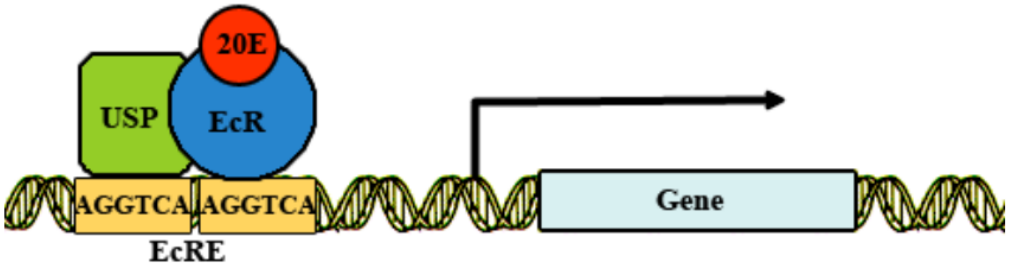

Figure 5. EcR/USP activation of ecdysone-induced genes. Ecdysone binds to the EcR/USP complex, which regulates its transcriptional activity. The EcR/USP complex is bound to promoter sequences called palindromic response elements (EcRE) (Notarangelo 2014).

Most larval tissues are destroyed during metamorphosis via PCD as a result of a rise in ecdysone, which is delivered during the first half-day of metamorphosis in two pulses (Lee et al.

2002). The first ecdysone pulse occurs at the end of the third instar larval stage (Bond et al. 2011; Lee et al. 2002). This pulse induces the transcription of the early genes that initiate metamorphosis and puparium formation, resulting in the transition to the prepupal stage, and signals PCD in the anterior muscles and the midgut (Bond et al. 2011; Lee et al. 2002). The second ecdysone pulse follows at 10 to 12 hours APF, triggering the transcriptional cascades that induce the transition from the prepupal stage to the pupal stage (Bond et al. 2011; Lee et al. 2002). In response to this pulse, adult head eversion is induced, and the larval salivary glands, a PCD-susceptible larval tissue, are destroyed via PCD (Lee et al. 2002). Furthemore, this second ecdysone pulse serves as the developmental signal regulating the dissociation and remodeling of the larval fat bodies (Bond et al. 2011; Nelliot et al. 2006).

ßFTZ-F1

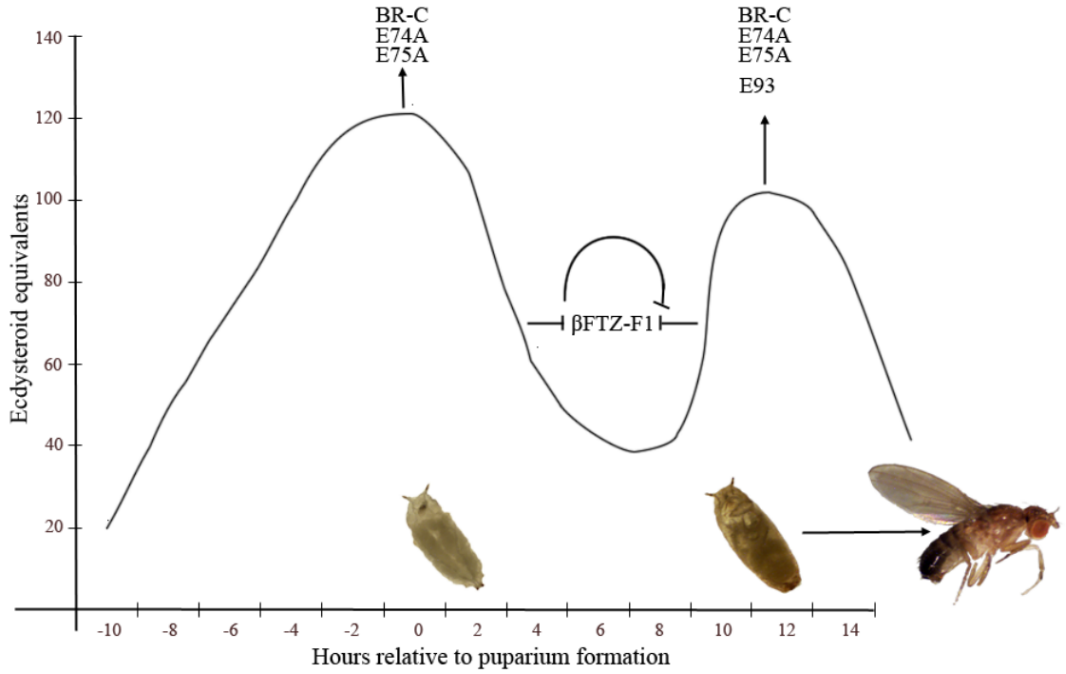

Figure 6. Timing of ecdysone pulses and expression of *ßFTZ-F1*. Ecdysone equivalents are plotted on the y-axis, versus hours relative to puparium formation on the x-axis. The initial ecdysone pulse peaks at 0 hours APF, inducing the transition to the prepupal stage. As it declines, *ßFTZ-F1* is expressed. The second ecdysone pulse peaks between 10 and 12 hours APF, inducing the transition to the pupal stage and metamorphosis (Notarangelo 2014).

The decline of the first pulse of ecdysone induces transcription of the mid-prepupal genes, one of which encodes the nuclear receptor *ßFTZ-F1* (Bond et al. 2011). *ßFTZ-F1* serves as a competence factor, necessary for modifying transcriptional programs in order to allow tissues to undergo stage-specific responses to the second ecdysone pulse (Bond et al. 2011; Lee et al. 2002; Yamada et al. 2000; Yamanaka et al. 2013; Zhu et al. 2006). Expression of *ßFTZ-F1* is regulated by several ecdysone-induced proteins, dependent upon the decline of the initial

ecdysone pulse (Bond et al. 2011). Two of these proteins, DHR3 and DHR4, regulate *ßFTZ-F1* via induction, while another, dBlimp-1, exhibits a repressive effect that is particularly critical in *ßFTZ-F1* regulation (Bond et al. 2011; Yamada et al. 2000). Transcriptional repression of *ßFTZ-F1* is a result of direct binding by dBlimp-1 at the promoter region (Bond et al. 2011). As dBlimp-1 is expressed in response to the initial ecdysone pulse and is degraded rapidly, it acts to alter the expression of *ßFTZ-F1* at a specific point in development, and it has been shown that the precise timing of this regulation is necessary for proper pupal development (Agawa et al. 2007; Bond et al. 2011). Pupal developmental events such as head eversion, extension of the legs and wings, and PCD of the larval salivary glands are all developmental events arising as a result of stage-specific ecdysone response due to transcriptional program modification by *ßFTZ-F1* (Bond et al. 2011). There is strong evidence that *ßFTZ-F1* acts as a competence factor in the stage-specific remodeling of the larval fat bodies, occurring in response to the second ecdysone pulse (Bond et al. 2011). *ßFTZ-F1* serves to increase the competence of the larval fat body cells to respond to the increase in MMP2 resulting from the second pulse of ecdysone (Bond et al. 2011).

ßFTZ-F1 has been found to be both necessary and sufficient in its role as a competence factor for the reintroduction of the early genes in response to the second ecdysone pulse, inducing larval salivary gland PCD as previously stated (Lee et al. 2002). The role of *ßFTZ-F1* as a competence factor arises from its interactions with cofactors that serve to modify ecdysone responses (Yamanaka et al. 2013). In one such interaction, *ßFTZ-F1* binds directly to the histone acetyltransferase p160/SRC, a cofactor of the EcR/USP complex (Bond et al. 2011; Yamanaka et al. 2013; Zhu et al. 2006). This interaction results in the recruitment of the p160/SRC cofactor to the EcR/USP complex in an ecdysone-dependent manner (Yamanaka et al. 2013; Zhu et al.

2006). A model for the molecular mechanisms of this interaction in insects was outlined in studies on the mosquito *Aedes aegypti*, where *ßFTZ-F1* was found to facilitate loading of the p160/SRC cofactor and the EcR/USP complex onto target promoters, enhancing activation of the target genes through local histone acetylation (Bond et al. 2011; Yamanaka et al. 2013; Zhu et al. 2006).

Diap1, Dronc, and the PCD Signaling Pathway

One of the key regulators of the *Drosophila melanogaster* PCD signaling pathway is the E3 ubiquitin ligase *Drosophila inhibitor of apoptosis-1*, or *Diap1* (Lee et al. 2002; Steller 2008; Yin & Thummel 2004). E3 ubiquitin ligases play an essential role in cell cycle regulation and cell division, recruiting and transferring the highly conserved protein ubiquitin to protein substrates (Teixeira & Reed 2013). E3 ubiquitin ligases are able to mediate the addition of both singular ubiquitin molecules and ubiquitin chains, and allow for the recruitment of specific substrates to targets, marking them for degradation by the 26S proteasome complex (Teixeira & Reed 2013). Additionally, *Diap1* belongs to a class of proteins called IAPs, or inhibitor of apoptosis proteins (Steller 2008). IAPs bind caspaces, a class of pro-apoptotic cysteine proteases, suppressing their PCD-inductive activity (Kumar & Doumanis 2000, Steller 2008). Caspases cleave protein substrates following an aspartate residue, and are typically present in an inactive (procaspase) form until activation by apoptotic signaling and subsequent proteolytic cleavages (Kumar & Doumanis 2000; Meier et al. 2000). Protein cleavage via activated caspases underlies many of the morphological and biochemical changes associated with apoptotic PCD (Lee et al. 2002). *Diap1* targets the apical caspase *Dronc*, promoting its degradation and thus acting as an inhibitor of unwanted PCD (Hawkins et al. 2000; Lee et al. 2002; Steller 2008; Yin & Thummel

2004). *Dronc* activation is known to be essential for PCD to occur, as its loss of function is associated with a decrease in necessary PCD; furthermore, it has been shown to interact with *drICE*, an effector caspase that has also been found to play an essential role in PCD (Fraser et al. 1997; Lee et al. 2002; Kumar & Doumanis 2000; Meier et al. 2000).

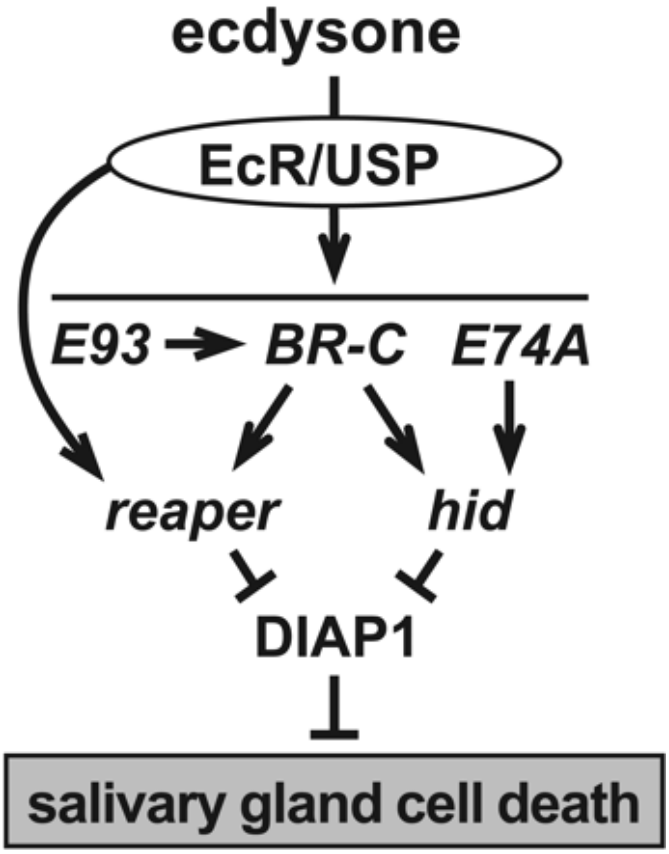

Figure 7. Regulation of the larval salivary gland PCD pathway. Ecdysone signaling is regulated through the EcR/USP complex. Ecdysone signaling induces the transcription-factor encoding genes, *BR-C*, *E74A*, and *E93,* which induce the death activator genes *reaper* and *hid*, and can also regulate *reaper* directly. The death activator genes inhibit the PDC inhibitor *Diap1*, allowing for PDC of the larval salivary glands (Yin & Thummel 2004).

The *Drosophila* PCD pathway is triggered by ecdysone-induced transcriptional activation of the death activator genes, *reaper (rpr), head involution defective (hid),* and *grim*, occurring with the second pulse of ecdysone (Lee et al. 2002; Steller 2008; Yin & Thummel 2004). These genes play an important role in the apoptosis of larval tissues at 12 hours APF, as *hid* expression

is necessary for triggering larval salivary gland death, and its cooperative function with *rpr* gives rise to PCD in the larval midgut (Yin & Thummel 2004). The death activator genes are IAP antagonists, functioning interchangeably to direct proteasome complex degradation from the caspaces to *Diap1* itself (Steller 2008; Yin & Thummel 2004). Transcription of the death activator genes is a stage-specific event requiring the ecdysone-induction of the transcription-factor encoding genes, *BR-C*, *E74A*, and *E93*, and relying on *ßFTZ-F1* as a competence factor (Lee et al. 2002; Yin & Thummel 2004). The death activator genes feature an N-terminal peptide motif, called the IAP-Binding Motif, or IBM (Steller 2008). These genes bind *Diap1* at the IBM, promoting its auto-ubiquitination and subsequent degradation (Hawkins et al. 2000; Steller 2008). The degradation of *Diap1* removes its inhibitory effect on *Dronc*, triggering caspase activation that induces PCD (Hawkins et al. 2000; Lee et al. 2002; Steller 2008; Yin & Thummel 2004). This signaling cascade is responsible for inducing larval salivary gland PCD and larval fat body dissociation/remodeling at 12 hours APF (Bond et al. 2011).

IV. Real-Time Quantitative Reverse Transcription Polymerase Chain Reaction

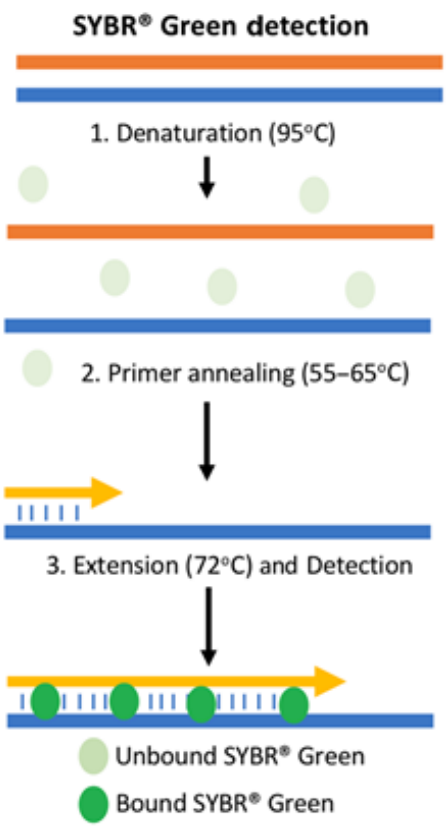

Figure 8. qRT-PCR with fluorescent dye. cDNA is denatured (1), primers are annealed (2), the cDNA is extended (3), and the fluorescent dye SYBR green is bound to the target products, allowing for detection via fluorescence levels. (Adams 2020).

Real-time quantitative reverse transcription PCR, or qRT-PCR, is a specialized polymerase chain reaction procedure that allows for the amount of PCR target products to be detected and measured during each cycle of PCR (Adams 2020; NCBI 2017). It is ideal for the investigation of gene expression in model systems (Adams 2020). One method for visualizing the level of a target present in a qRT-PCR product is through the use of a fluorescent dye, typically SYBR Green, designed to bind to double-stranded DNA (Adams 2020). The fluorescent dye will intercalate with qRT-PCR products as they are synthesized, emitting a fluorescent signal that may be used to determine how much of a target product is being produced

(Adams 2020). The brightness of the fluorescence is measured; the more of a target that is generated, the brighter the fluorescence will be (Adams 2020).

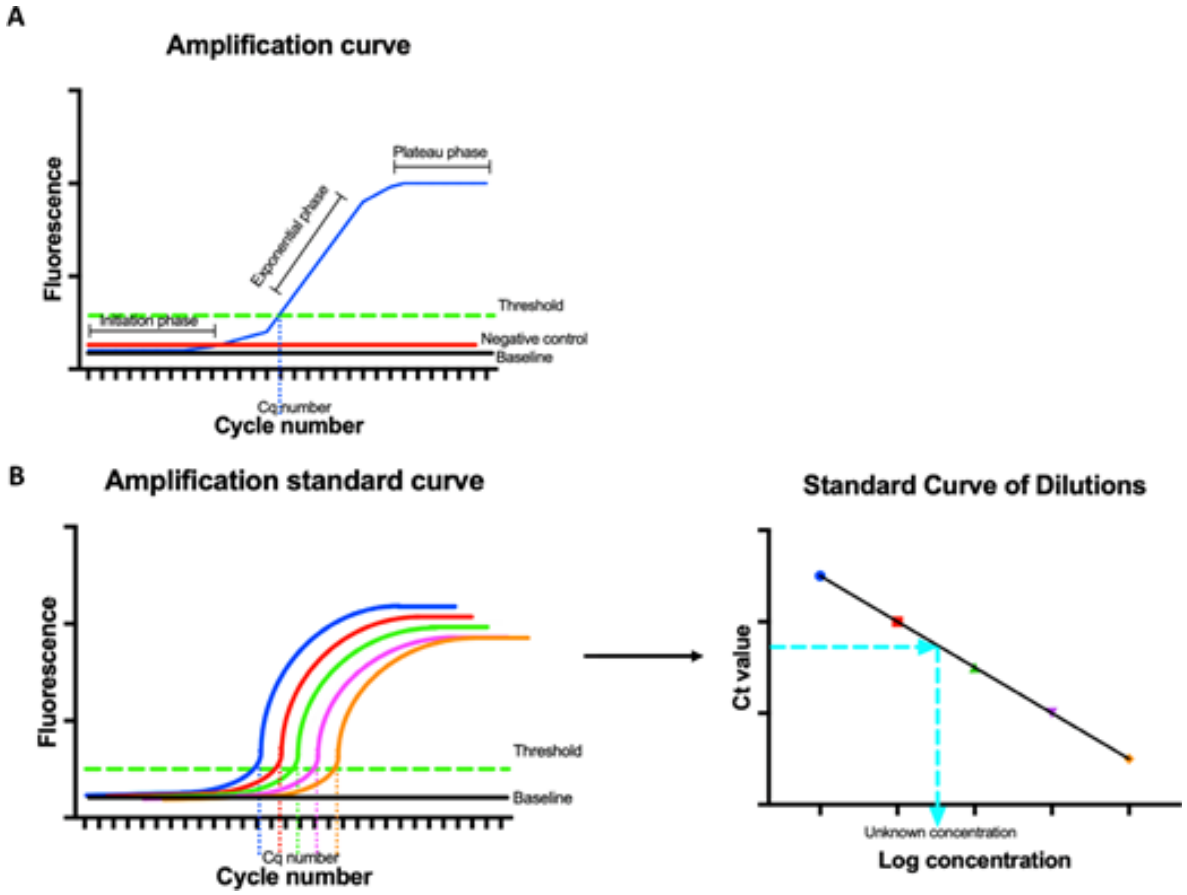

Figure 9. qRT-PCR quantitation. (A) Amplification curve generated in real time during qRT-PCR. The level of fluorescence during amplification is represented by the blue amplification curve. The threshold level, shown by the green line, represents the point at which fluorescence can be detected. The baseline, represented by the black line, shows the level of fluorescence during the phase before amplification (initiation phase). A negative control is shown in red. (B) Amplification curves are generated using serial dilution of standards of known concentrations. The point at which fluorescence levels cross the threshold is recorded as the Ct or Cq value, which is plotted against the log of the standard concentrations to generate a standard curve. The cyan line shows the relationship between Ct value and log of concentration; using this curve, one may be used to calculate the other (Adams 2020).

Levels of fluorescence in qRT-PCR are graphed as an amplification curve (Adams 2020). The level of fluorescence at the start of amplification is referred to as the initiation phase, and is

used as a baseline for fluorescence levels of the target in question (Adams 2020). This baseline level is below the limits of detection of the measuring instrument (NCBI 2017). The threshold level marks the point during amplification, referred to as the exponential phase, at which the level of fluorescence can be detected (Adams 2020; NCBI 2017). The first point at which a sample is detected above the threshold is recorded as the threshold cycle (Ct or Cq) value, forming the basis for quantitation (Adams 2020; NCBI 2017). As qRT-PCR is used to investigate targets whose expression levels may undergo change during biological processes, a gene whose expression is constant under the relevant biological conditions is selected as a reference gene, functioning as a positive control (Adams 2020). Housekeeping genes, required for cellular function, tend to make for ideal reference genes, as they are expressed consistently in all of an organism's cells (Adams 2020). There are a couple methods of quantitation, the most useful of which when working with known concentrations is absolute quantitation (Adams 2020). In absolute quantitation, Ct values for each target are graphed on the y-axis against the logs of their respective concentrations of cDNA on the x-axis, generating a standard curve (Adams 2020; Enke 2016). The slope of the standard curve for each target can then be used to calculate its primer efficiency (Enke 2016).

V. Findings of Previous Experiments

A 2019 project done by Ashley Han aimed to examine the roles of *Diap1* and *Dronc* in PCD during *Drosophila melanogaster* metamorphosis (Han 2019). Using qRT-PCR, the study aimed to determine the relative expression levels of *Diap1* and *Dronc* in larval fat bodies, noted for their resistance to PCD, to those in the larval salivary glands, another type of larval tissue that is known to undergo PCD (Han 2019). The study used w^{1118} (white-eyed, but otherwise

wild-type) *Drosophila melanogaster* as an experimental subject, and the housekeeping gene *Actin 5c* as a reference gene (Han 2019).

While the presence of both *Diap1* and *Dronc* in the samples was confirmed, and calculation of primer efficiencies found that they were acceptable at between 96% and 106%, the absence of viable control data prevented this study from reaching a conclusion (Han 2019). cDNA from the larval salivary glands to be used in the procedure was missing; while qRT-PCR was able to be performed on larval fat body cDNA, relative levels of expression were undeterminable without data from the larval salivary glands for comparison (Han 2019).

VI. Hypothesis and Goals of this Study

The goal of this study is to follow up on Ashley Han's 2019 study, hypothesizing that up-regulation of *Dronc* and down-regulation of *Diap1* would promote PCD in *Drosophila melanogaster,* and that, in PCD-resistant larval fat bodies, there is likely an up-regulation of *Diap1* and a down-regulation of *Dronc* (Han 2019). It is expected that comparison of the relative levels of *Diap1* and *Dronc* will reveal lower levels of *Diap1* in the larval salivary glands and higher levels of *Diap1* in the larval fat bodies, and, conversely, higher levels of *Dronc* in the larval salivary glands and lower levels of *Diap1* in the larval fat bodies. In this study, I aim to further scientific understanding of how the PCD pathway is regulated by *Diap1* and *Dronc*, and hope that it might contribute more broadly to research into treatment of diseases underlined by misregulation of PCD.

Materials and Methods: Preliminary Research

In order to prepare to perform the research necessary to test this hypothesis, several protocols were performed to test the quality of the materials used and hone the necessary techniques. Stocks *of Drosophila melanogaster* w^{1118} were raised on standard fly food and stored at 25°C, and were used as subjects in these experiments.

I. RNA Isolation

Larval fat bodies were collected from seven third instar larvae, placed in approximately 30 µl of aqueous buffer for RNA isolation, combined with TRIzol, and homogenized. The samples were labeled 10/22 in accordance with the date on which they were collected. These samples were held at -80°C until next steps were ready to be taken.Larval fat bodies were collected from six third instar larvae and placed in approximately 30 µl of aqueous buffer for RNA isolation. These samples were held at -80°C overnight, thawed, combined with TRIzol, and homogenized. The samples were labeled 10/31 in accordance with the date on which they were collected.

2 mL Phase Lock Gel-Heavy tubes were spun at 12,000 rpm for 1 minute. Samples were transferred to these tubes, 60 µl of chloroform was added, and the tubes were shaken by hand. Samples were centrifuged at 12,000 rpm for 10 minutes at 2-8°C. As phasing appeared up to expectation, each sample was transferred to a clean tube, labeled with its collection date, and combined with 160 µl of isopropanol. Samples were thoroughly mixed, then allowed to precipitate at -20°C overnight. The following day, samples were cold centrifuged at 4°C for 30 minutes at 13.4 rpm. A 75% ethanol solution was made up, supernatant was pipetted off of the

samples, and pellets were rinsed in 500 µl of the ethanol solution. Next, 10/22 was spun at full speed for a total of 20 minutes, and 10/31 was spun at full speed for 10 minutes. Supernatant was thoroughly pipetted off. Pellets were allowed to dry for between 1 to 2 minutes, then were redissolved in 5 µl of nucleotide-free water and incubated for 10 minutes at approximately 60°C. Samples were allowed to sit at room temperature for 5 additional minutes, then were held in storage at -80°C until the results of the RNA isolation could be analyzed. Once ready for analysis, the samples were dethawed, and analyzed using a nanodrop spectrometer. Samples were then stored at -80°C for future use in cDNA synthesis.

II. First-Strand cDNA Synthesis

RNA isolated in the previous step was used in the synthesis of cDNA. No negative control was made during this procedure. Sample tubes were labeled in accordance with the collection date of the original sample from which the RNA was isolated (10/22 and 10/31). A master mix was prepared in accordance with Table 1, with one tube made up for the 10/22 RNA and another tube made up for the 10/31 RNA.

Table 1. Master mix 1 reagents for cDNA synthesis.

Component	Amount per Reaction
RNA	1 µl
10 mM dNTP mix	1 µl
0.5 µg/µl oligo (dt) primer	1 µl
DEPC-treated water	7 µl

Two reactions worth of master mix, sans RNA, were prepared. One reaction worth of master mix was measured out for combination in a tube with the appropriate amount of each respective RNA

sample. These materials were combined in a tube, and incubated at 65°C for 5 minutes, then placed on ice. Two reactions' worth of a second master mix was prepared in a separate tube, in accordance with Table 2.

Table 2. Master mix 2 reagents for cDNA synthesis.

Component	Amount per Reaction
10X RT buffer	2 µl
25 mM $MgCl_2$	4 µl
0.1 M DDT	2 µl
RNaseOUT (40 U/µl)	1 µl

9 µl of master mix 2 was combined and mixed with each prepared tube of RNA and master mix 1, and briefly centrifuged for collection of components. The rection was incubated for two minutes at 42°C. 1 µl of SuperScript™ II RT was added to each tube. The reaction was incubated at 42°C for 50 minutes, then terminated at 70°C for 15 minutes. Tubes were stored at -80°C until the procedure could be completed. The components were then thawed, and tubes were briefly centrifuged to collect their contents. 1 µl of RNase H was added to each tube. The tubes were incubated at 37°C for 20 minutes. Upon completion of the procedure, tubes were stored at -20°C for future use in PCR and gel electrophoresis.

III. Reverse Transcriptase PCR and Gel Electrophoresis

Forward and reverse primers for *Diap1* and *Dronc*, serving as experimental genes, and *Actin 5c*, a housekeeping gene serving as a positive control, were diluted to 10 µM for use. Primers were designed by Ashley Han, and are detailed in Table 3. Six total reactions were prepared: One for each of the three genes in question, using cDNA prepared from samples

collected either on 10/22 or 10/31. The reactions were labeled according to the schema visualized in Table 4.

Table 3. Forward and reverse primer sequences for *Diap1*, *Actin 5c*, and *Dronc*. (Han 2019).

Gene	Primer ID	Sequence
Diap1	Forward	5'-CGG TTT ATC CAT TGC TCG AT-3'
Diap1	Reverse	5'-TCT GGC TCC TTT CCT CTG AA-3'
Actin 5c	Forward	5'-TCT ACG AGG GTT ATG CCC TT-3'
Actin 5c	Reverse	5'-GCA CAG CTT CTC CTT GAT GT-3'
Dronc	Forward	5'-ATT GCA CTG CGC AAT ATC AA- 3'
Dronc	Reverse	5'-CCA CAT AAG GGG TGA GTG CT- 3'

RT-PCR master mix was prepared for each reaction according to Table 4, utilizing the appropriate forward and reverse primers for each.

Table 4. Reagents for RT-PCR.

Component	Amount per Reaction
10X PCR Buffer-$MgCl_2$ (sans $MgCl_2$)	5 µl
50 µM $MgCl_2$	3 µl
10 mM dNTPs	1 µl
10 µM forward primer	2 µl
10 µM reverse primer	2 µl
cDNA	2 µl
Nuclease-free water	34.6 µl
Taq Polymerase	0.4 µl

The cDNA samples were then amplified using Reverse-Transcriptase Polymerase Chain Reaction (RT-PCR). A preset thermocycler program saved as *diap1primerset1* was run to perform the RT-PCR. The thermocycler profile of this program is outlined in Table 5.

Table 5. RT-PCR Thermocycler profile for program *diap1primerset1.*

Stage	Temperature	Duration	Cycle Count
Denaturation	94°C	30 seconds	
Annealing	60.2°C	30 seconds	35
Extension	72°C	30 seconds	
Final Extension	72°C	5 minutes	1
Final Hold	4°C	Indefinite	

A 1.6% Agarose gel was prepared with 1X TAE buffer, with gel red added as a fluorescent tag so that the cDNA could be visualized under UV light. 2 µl of loading dye was added to each sample, and 20 µl of each sample was loaded into the gel. 10 µl of 100bp ladder was also loaded into the gel for reference. The gel was run for 30 minutes, and imaged using a Fujifilm

LAS-3000 Luminescence Image Analyzer on UV365 with autoexposure on. Gel images were saved for analysis.

Results

I. RNA Isolation

Isolated RNA was analyzed for purity using a nanodrop spectrometer. The 260/280 ratio is used to detect protein contamination, and the 260/230 ratio is used to detect numerous contaminants that absorb at 230 nm (Koetsier and Cantor 2019). These ratios can be used as an indication of the purity of an RNA sample. Pure RNA has a 260/280 ratio of approximately 2.1 or greater, and a 230/260 ratio of 1.8 or greater (Koetsier and Cantor 2019). Sample 10/22 had a 260/280 ratio of 2.06, and a 260/230 ratio of 1.26. Sample 10/32 had a 260/280 ratio of 1.93, and a 260/230 ratio of 0.64. These values do not indicate perfectly pure RNA, but they do show that the samples are sufficiently clean for use in cDNA synthesis.

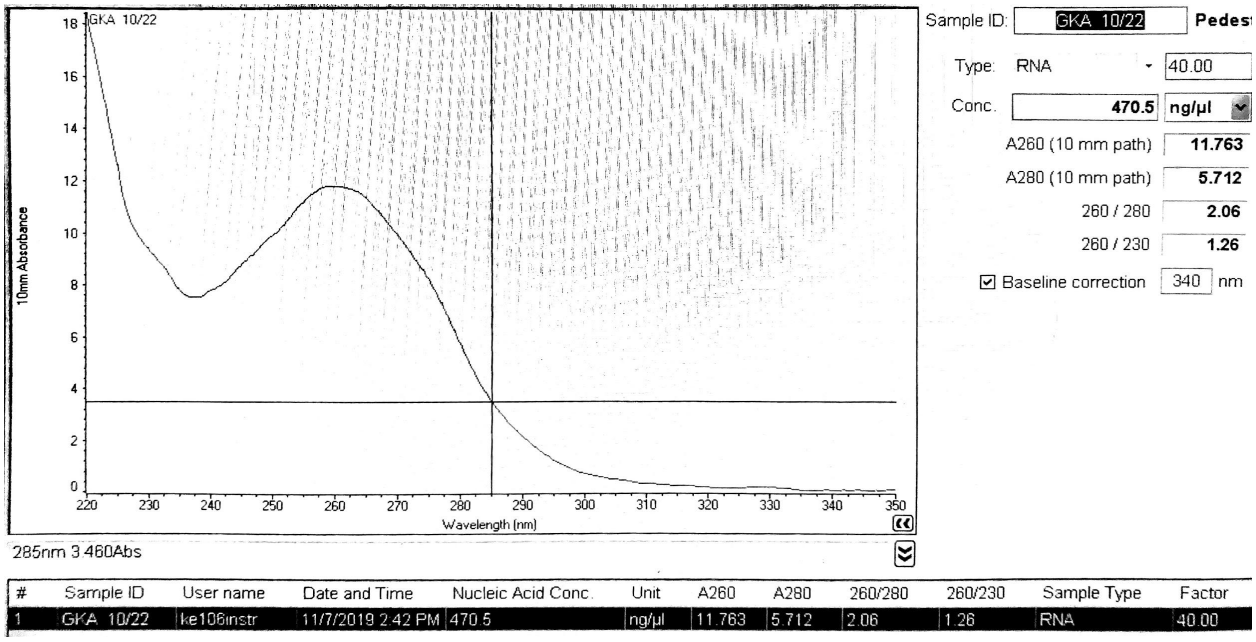

Figure 11. 10mm Absorbance vs. Wavelength in nm for RNA sample 10/22. Nucleic Acid Concentration is displayed to be 470.5 ng/µl, 260/280 ratio is displayed to be 2.06, and 260/230 ratio is displayed to be 1.26.

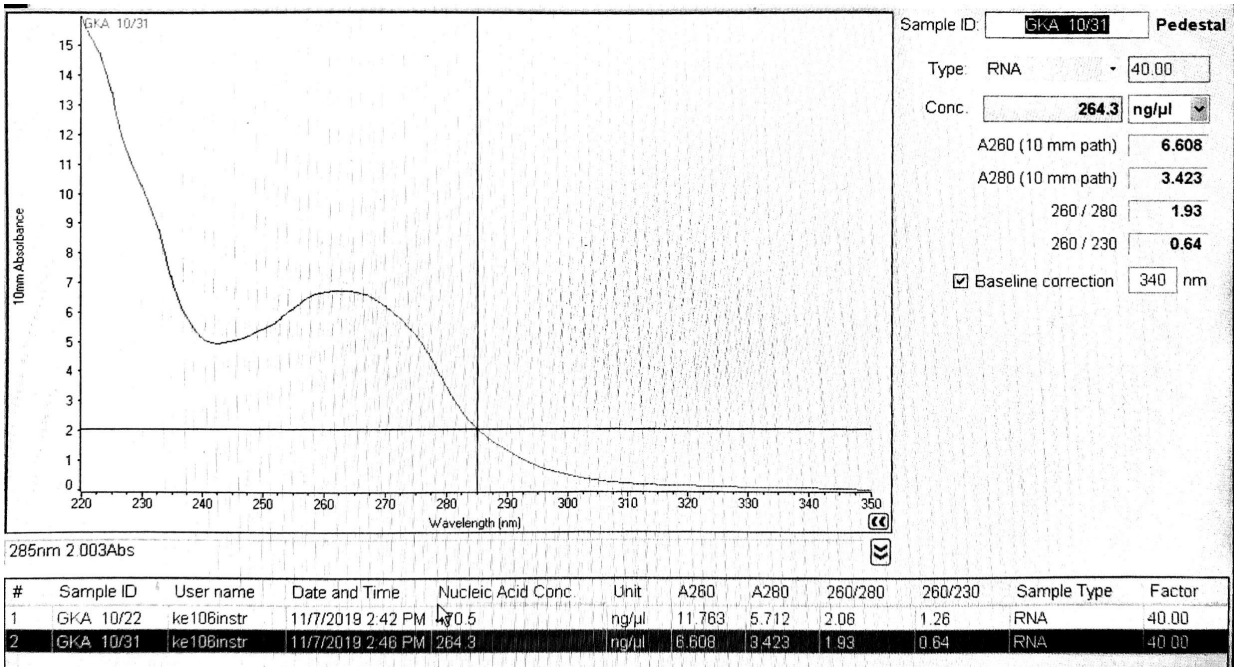

Figure 12. 10mm Absorbance vs. Wavelength in nm for RNA sample 10/31. Nucleic Acid Concentration is displayed to be 264.3 ng/µl, 260/280 ratio is displayed to be 1.93, and 260/230 ratio is displayed to be 0.64.

II. Gel Electrophoresis

Gel electrophoresis was performed on samples amplified via RT-PCR expressing *Diap1*, *Actin 5c*, and *Dronc* transcripts, isolated from fat bodies of *Drosophila melanogaster* w^{1118} third instar larvae (Figure 3). *Diap1* bands were formed below size 150bp and *Dronc* bands appeared around 200bp, as expected, indicating their expression. Used as a positive control, *Actin 5c* bands are visible around size 150bp, indicating its expression and confirming the success of the RT-PCR procedure. Visible in each lane below the bands indicating the presence of the RT-PCR target products are "primer dimer" bands, formed by unincorporated primers.

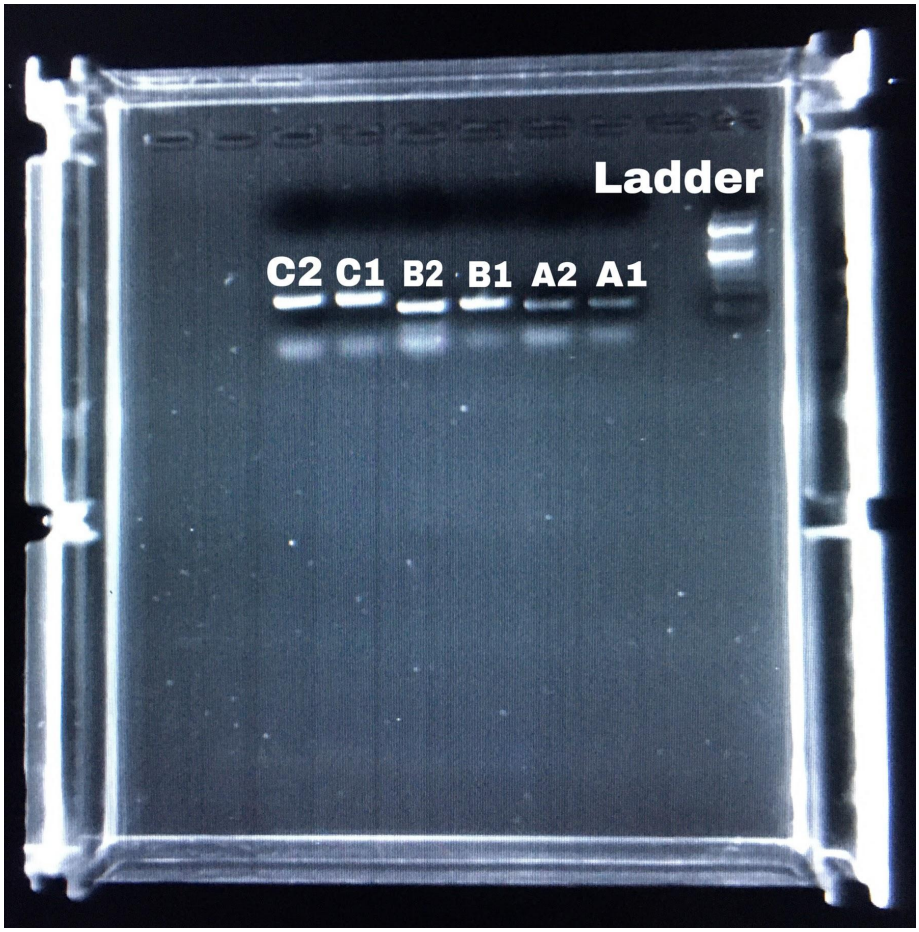

Figure 13. Gel electrophoresis of *Drosophila melanogaster* w^{1118} cDNA amplified with *Dronc* (C), *Actin 5c* (B), and *Diap1* (A) primers from samples 10/22 (1) and 10/31 (2). The righthandmost lane is loaded with a 100bp ladder. Bands A1 and A2, slightly beneath size 150bp, indicate the presence of *Diap1* in samples 10/22 and 10/31, respectively. Bands B1 and B2, around size 150bp, indicate the presence of *Actin 5c* in samples 10/22 and 10/31, respectively. Bands C1 and C2, at size 200bp, indicate the presence of *Dronc* in samples 10/22 and 10/31, respectively. No negative control was run.

Discussion

I. Preliminary Research

These experiments prepared for future investigation into the roles of *Dronc* and *Diap1* in PCD of larval fat bodies in *Drosophila melanogaster*. The success of the RT-PCR of the synthesized cDNA and subsequent gel electrophoresis demonstrates that the primers diluted for use in this experiment are working properly, and that all materials and techniques are up to high enough standard that further experimentation is ready to be performed.

II. Current and Continuing Research

At this juncture, experimentation has proceeded on *Drosophila melanogaster* w^{1118} pupae aged 12 hours APF. A total of 11 pupae were collected at 0 hours APF over the course of 24 minutes, and aged for 12 hours from the start of the collection process. At 12 hours APF, larval fat bodies were collected from 6 pupae, and larval salivary glands were collected from five pupae; the dissection process took a total of 1 hour and 44 minutes. The collected materials have been homogenized in TRIzol, and are to undergo RNA isolation, cDNA synthesis, RT-PCR, and qRT-PCR. Concerns include the long dissection time as well as difficulties with laboratory equipment, though the latter has largely been troubleshot. Primers will target *Diap1*, *Dronc*, and, as a reference gene, *Actin 5c*, and a negative control will be included in order to further ensure the accuracy of any results.

Via qRT-PCR, this study intends to compare the level of *Diap1* expression to the level of *Dronc* expression in each of these larval tissues, and compare these levels of expression relative to one another across the tissue types in question. Successful results will provide insight into how

and if *Diap1* and *Dronc* are regulated differently in the larval salivary glands, which do undergo PCD, versus in the larval fat bodies, which do not.

III. Conclusion

Understanding the mechanical underpinnings of the PCD pathway has potential in the further development of treatments for health conditions arising from the dysregulation thereof. Expanding scientific knowledge of apoptotic triggers and the factors with which they interact might lead to the improved targeting of PCD inducers and inhibitors, a method of treatment long in question in studies of cancer and neurodegenerative diseases. The importance of apoptotic pathways in the development of cancer treatments is becoming increasingly clear, as the current gold-standard treatment, chemotherapy, has already been found to function by inducing PCD in malignant anti-apoptotic tumors (Chen & Lai 2009). Further understanding of the cell death pathway and its components could lead to greater and improved means of apoptotic induction in malignant PCD-resistant tumors; and, conversely, an understanding of what effectors might best be blocked to prevent the progression of various PCD-linked neurodegenerative diseases (Chen & Lai 2009; Mattson 2000). In addition to shedding light on what components may make for viable treatment targets, the effectiveness of these potential treatments may also be more accurately projected. As such, there have been extensive efforts to research apoptotic triggers in human cancer cells. Apoptotic regulators have been identified in cancers of many human tissues; however, it is often the case that these regulators vary across tissue types (Chen & Lai 2009). A unifying model, as could potentially be provided by research on *Drosophila melanogaster,* may be useful in better identifying common points between these pathways for treatment development (Chen & Lai 2009).

This study aims to improve scientific understanding of the mechanical underpinnings of the PCD pathway, investigating the interactions of its known effectors in normally apoptotic and biologically regulated anti-apoptotic tissues.This knowledge may serve as a model for the interactions of evolutionarily conserved homologs in human PCD pathways, and could inform which effectors may be investigated for targeting in the potential treatments discussed. Overall, this study hopes that its hypotheses and potential results might contribute to scientific knowledge of the PCD pathway and its effectors, furthering an understanding critical to advancements in healthcare research.

Appendix

Table 6. Labeling schematic for RT-PCR tubes. Tubes were lettered according to the gene they would be detecting, and numbered according to the date on which the samples they were synthesized from were collected.

	10/22	**10/31**
Diap1	A1	A2
Actin 5c	B1	B2
Dronc	C1	C2

Literature Cited

Adams, G. (2020). A beginner's guide to RT-PCR, qPCR and RT-qPCR. *The Biochemist*, *42*(3), 48–53. https://doi.org/10.1042/bio20200034

Agawa, Y., Sarhan, M., Kageyama, Y., Akagi, K., Takai, M., Hashiyama, K., Wada, T., Handa, H., Iwamatsu, A., Hirose, S., & Ueda, H. (2007). Drosophila Blimp-1 Is a Transient Transcriptional Repressor That Controls Timing of the Ecdysone-Induced Developmental Pathway. *Molecular and Cellular Biology*, *27*(24), 8739–8747. https://doi.org/10.1128/mcb.01304-07

Aguila, J. R., Suszko, J., Gibbs, A. G., & Hoshizaki, D. K. (2007). The role of Larval fat cells in adult Drosophila melanogaster. *Journal of Experimental Biology*, *210*(6), 956–963. https://doi.org/10.1242/jeb.001586

Austin, C. P. (n.d.). *Apoptosis*. National Human Genome Research Institute. https://www.genome.gov/genetics-glossary/apoptosis.

Bond, N. D., Nelliot, A., Bernardo, M. K., Ayerh, M. A., Gorski, K. A., Hoshizaki, D. K., & Woodard, C. T. (2011). ßFTZ-F1 and Matrix metalloproteinase 2 are required for fat-body remodeling in Drosophila. *Developmental Biology*, *360*(2), 286–296. https://doi.org/10.1016/j.ydbio.2011.09.015

Chen, G. G., & Lai, P. B. S. (2009). *Apoptosis in Carcinogenesis and Chemotherapy Apoptosis in Cancer*. Springer Netherlands. https://doi.org/978-1-4020-9597-9

Enke, R. (2016). qPCR Primer Efficiency Standard Curve Analysis. *CSHL DNALC RNA-Seq for the Next Generation Working Group*.

Fernández-Moreno, M. A., Farr, C. L., Kaguni, L. S., & Garesse, R. (2007). Drosophila melanogaster as a model system to study mitochondrial biology. *Methods in Molecular Biology*, 33–49. https://doi.org/10.1007/978-1-59745-365-3_3

Fraser, A. G. (1997). drICE is an essential caspase required for apoptotic activity in Drosophila cells. *The EMBO Journal*, *16*(20), 6192–6199. https://doi.org/10.1093/emboj/16.20.6192

Han, A. (2019). The Role of the Caspase Dronc and Inhibitor of Apoptosis (Diap1) in Programmed Cell Death (PCD) of Drosophila melanogaster. *Mount Holyoke College*.

Hawkins, C. J., Yoo, S. J., Peterson, E. P., Wang, S. L., Vernooy, S. Y., & Hay, B. A. (2000). The Drosophila Caspase DRONC Cleaves following Glutamate or Aspartate and Is Regulated by DIAP1, HID, and GRIM. *Journal of Biological Chemistry*, *275*(35), 27084–27093. https://doi.org/10.1016/s0021-9258(19)61483-3

Jennings, B. H. (2011). Drosophila – a versatile model in biology & medicine. *Materials Today*, *14*(5), 190–195. https://doi.org/10.1016/s1369-7021(11)70113-4

Koetsier, G., & Cantor, E. (2019). A Practical Guide to Analyzing Nucleic Acid Concentration and Purity with Microvolume Spectrophotometers. *New England Biolabs, Inc*.

Kroemer, G., El-Deiry, W. S., Golstein, P., Peter, M. E., Vaux, D., Vandenabeele, P., Zhivotovsky, B., Blagosklonny, M. V., Malorni, W., Knight, R. A., Piacentini, M., Nagata, S., & Melino, G. (2005). Classification of cell Death: Recommendations of the Nomenclature Committee on cell death. *Cell Death & Differentiation*, *12*(S2), 1463–1467. https://doi.org/10.1038/sj.cdd.4401724

Kumar, S., & Doumanis, J. (2000). The fly caspases. *Cell Death & Differentiation*, *7*(11), 1039–1044. https://doi.org/10.1038/sj.cdd.4400756

LaFerla, F. M., Tinkle, B. T., Bieberich, C. J., Haudenschild, C. C., & Jay, G. (1995). The Alzheimer's aβ peptide induces neurodegeneration and apoptotic cell death in transgenic mice. *Nature Genetics*, *9*(1), 21–30. https://doi.org/10.1038/ng0195-21

Lee, C.-Y., Simon, C. R., Woodard, C. T., & Baehrecke, E. H. (2002). Genetic mechanism for the stage- and tissue-specific regulation of steroid triggered programmed cell death in drosophila. *Developmental Biology*, *252*(1), 138–148. https://doi.org/10.1006/dbio.2002.0838

Mattson, M. P. (2000). Apoptosis in neurodegenerative disorders. *Nature Reviews Molecular Cell Biology*, *1*(2), 120–130. https://doi.org/10.1038/35040009

McGill, G., & Fisher, D. E. (1997). Apoptosis in tumorigenesis and cancer therapy. *Frontiers in Bioscience*, *2*(4), d353–379. https://doi.org/10.2741/a197

Meier, P., Silke, J., Leevers, S. J., & Evan, G. I. (2000). The Drosophila caspase Dronc is regulated by DIAP1. *The EMBO Journal*, *19*(4), 598–611. https://doi.org/10.1093/emboj/19.4.598

Miller, J. M., Oligino, T., Pazdera, M., López, A. J., & Hoshizaki, D. K. (2002). Identification of fat-cell enhancer regions in Drosophila melanogaster. *Insect Molecular Biology*, *11*(1), 67–77. https://doi.org/10.1046/j.0962-1075.2001.00310.x

Mochizuki, H., Goto, K., Mori, H., & Mizuno, Y. (1996). Histochemical detection of apoptosis in Parkinson's disease. *Journal of the Neurological Sciences*, *137*(2), 120–123. https://doi.org/10.1016/0022-510x(95)00336-z

Nakagawa, Y., & Sonobe, H. (2016). 20-Hydroxyecdysone. *Handbook of Hormones*, 560–563. https://doi.org/10.1016/b978-0-12-801028-0.00238-5

Nelliot, A., Bond, N., & Hoshizaki, D. K. (2006). Fat-Body Remodeling in Drosophila melanogaster. *Genesis*, *44*(8), 396–400. https://doi.org/10.1002/dvg.20229

Notarangelo, G. (2014). The Role of βFTZ-F1 and MMP2 in Regulating Hormone-Mediated Autophagy and Insulin Signaling in the Drosophila Fat Body. *Mount Holyoke College*.

Steller, H. (2008). Regulation of apoptosis in drosophila. *Cell Death & Differentiation*, *15*(7), 1132–1138. https://doi.org/10.1038/cdd.2008.50

Teixeira, L. K., & Reed, S. I. (2013). Ubiquitin Ligases and Cell Cycle Control. *Annual Review of Biochemistry*, *82*(1), 387–414. https://doi.org/10.1146/annurev-biochem-060410-105307

U.S. National Library of Medicine. (2017). *Real-Time qRT-PCR*. National Center for Biotechnology Information. https://www.ncbi.nlm.nih.gov/probe/docs/techqpcr/.

U.S. National Library of Medicine. (2021). *20-Hydroxyecdysone*. National Center for Biotechnology Information. PubChem Compound Database. https://pubchem.ncbi.nlm.nih.gov/compound/20-Hydroxyecdysone.

Yamada, M., Murata, T., Hirose, S., Lavorgna, G., Suzuki, E., & Ueda, H. (2000). *Temporally restricted expression of transcription factor betaFTZ-F1: significance for embryogenesis, molting and metamorphosis in Drosophila melanogaster.* Development (Cambridge, England). https://pubmed.ncbi.nlm.nih.gov/11060234/.

Yamanaka, N., Rewitz, K. F., & O'Connor, M. B. (2013). Ecdysone Control of Developmental Transitions: Lessons from Drosophila Research. *Annual Review of Entomology*, *58*(1), 497–516. https://doi.org/10.1146/annurev-ento-120811-153608

Yin, V. P., & Thummel, C. S. (2004). A balance between the diap1 death inhibitor and reaper and hid death inducers controls steroid-triggered cell death in drosophila. *Proceedings of the National Academy of Sciences*, *101*(21), 8022–8027. https://doi.org/10.1073/pnas.0402647101

Zhu, J., Chen, L., Sun, G., & Raikhel, A. S. (2006). The Competence Factor βFtz-F1 Potentiates Ecdysone Receptor Activity via Recruiting a p160/SRC Coactivator. *Molecular and Cellular Biology*, *26*(24), 9402–9412. https://doi.org/10.1128/mcb.01318-06